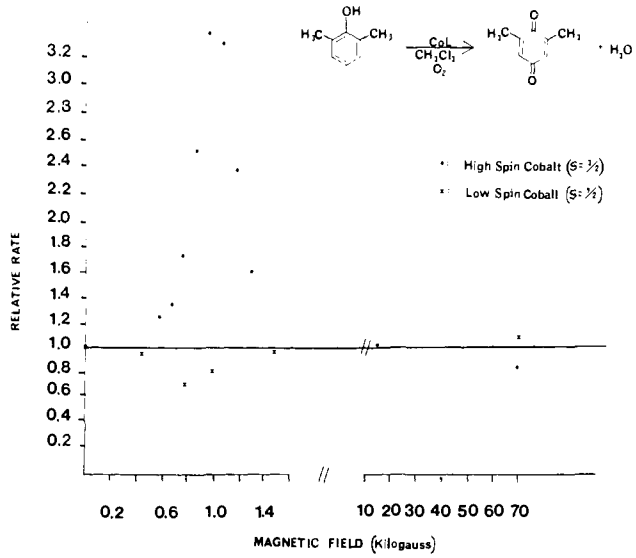

Figure 1. The effect of a magnetic field on the relative rate, k(rel), in the catalytic oxidation of 2,6-dimethylphenol by high spin CoSMDPT ($S = {}^3/_2$) and low spin Co(SALEN)(py) ($S = {}^1/_2$).

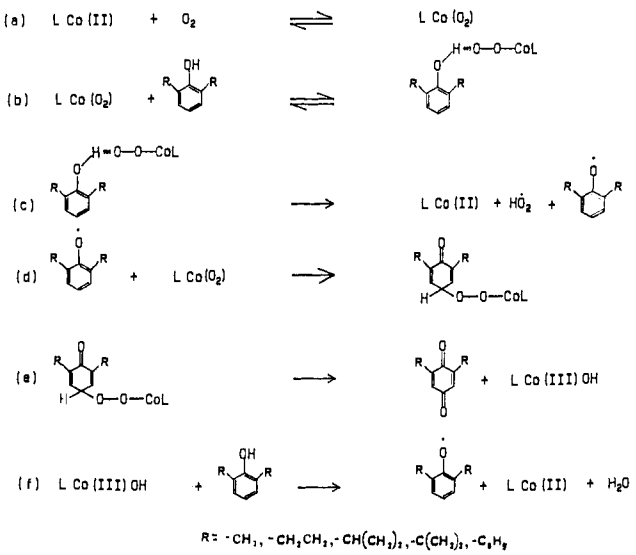

Figure 2. A mechanistic scheme for the catalytic oxidation of 2,6-dimethylphenol by a cobalt(II) Schiff-base complex. L constitutes five of the donor atoms in SMDPT or SALEN(py).

involves electron transfer between two diamagnetic species, $LCo^{III}OH$ and 2,6-dimethylphenol. Since the formation of the phenoxy radical ($S = {}^1/_2$), Co^{II}SALEN(py) ($S = {}^1/_2$) or Co^{II}SMDPT ($S = {}^3/_2$), and H_2O involves a different net change in electron spin angular momentum, it is not unreasonable to expect different magnetic field effects.

The k(rel) versus H profile in Figure 1 indicates that the magnetic field effect in these reactions is the consequence of at least two mechanisms which manifest opposite magnetic field effects.[6] One mechanism involves an electronic Zeeman effect which induces mixing between states with different electron spin multiplicities. It is proportional to the magnetic field strength and Δg, the difference in the g values of the unpaired electrons in the reaction pair. This effect is balanced by a hyperfine coupling mechanism which is most effective when $H = -2J/\Delta g\beta$, where $-2J$ is the electron spin-spin coupling and β is the electronic Bohr magneton. The magnetic field effects for the high- and low-spin cobalt(II) catalysts is the sum of the relative contributions of these two intersystem crossing processes which occur during the electron-transfer step (f).

The difference in the magnetokinetics of high-spin Co^{II}SMDPT and low-spin Co^{II}SALEN can be understood from existing theory developed to interpret magnetic field effects in singlet-triplet (S-T) radical pair[6] and triplet-triplet (T-T) annihilation reactions.[7] The catalyst regeneration step (f) is thought to involve the initial encounter of diamagnetic $LCo^{III}OH$ and 2,6-dimethylphenol, the transfer of an electron to form a singlet state radical pair, followed by intersystem crossing to produce the products, H_2O, LCo^{II}, and the phenoxy radical. The back reaction is spin forbidden once intersystem crossing to an electronic state with higher spin multiplicity has occurred. It follows that for Co^{II}SALEN, where a weak magnetic field inhibits the formation of the triplet state products, the transmission coefficient for step (f) is influenced by the rate of intersystem crossing between the singlet and triplet states, a rate that depends upon the degree of S-T mixing in the low-spin cobalt(II)-phenoxy radical pair. In contrast, Co^{II}SMDPT accelerates the reaction rate in a weak magnetic field. Because a high spin cobalt(II)-phenoxy radical forms a quintet-triplet state pair,[8] quantum mechanical mixing with a singlet state potential energy surface further along the reaction coordinate is precluded. We believe the difference in the magnetokinetics of high- and low-spin cobalt(II) complexes is explained in these terms.

(6) (a) Closs, G. L.; Doubleday, C. E. *J. Am. Chem. Soc.* **1973**, *95*, 2735. (b) Turro, N. J.; Kraeutler, B. *Acc. Chem. Res.* **1980**, *13*, 369. (c) Gould, I. R.; Turro, N. J.; Zimmt, M. B. *Adv. Phys. Org. Chem.* **1984**, *20*, 1. (d) Hata, N. *Bull. Chem. Soc. Jpn.* **1985**, *58*, 1088. (e) Tanimoto, Y.; Takayama, M.; Itoh, M.; Nakagaki, R.; Nagakura, S. *Chem. Phys. Lett.* **1986**, *129*, 414. (f) Turro, N. J.; Chow, M. F.; Chung, C. J.; Kraeutler, B. *J. Am. Chem. Soc.* **1980**, *102*, 4843 and references therein. (g) Atkins, P. W.; Lambert, T. P. *Ann. Rep. Chem. Soc. A* **1975**, *67*, and references therein. (h) Zimmt, M. B.; Doubleday, C.; Turro, N. J. *J. Am. Chem. Soc.* **1985**, *107*, 6724. (i) Zimmt, M. B.; Doubleday, C.; Gould, C.; Turro, N. J. *J. Am. Chem. Soc.* **1985**, *107*, 6726. (j) Hayashi, H.; Nagakura, S. *Bull. Chem. Soc. Jpn.* **1978**, *51*, 2862. (k) Sakaguchi, Y.; Hayashi, H.; Nagakura, S. *Bull. Chem. Soc. Jpn.* **1980**, *53*, 39. (l) Hayashi, H.; Nagakura, S. *Bull. Chem. Soc. Jpn.* **1984**, *57*, 322. (m) Turro, N. J.; Zimmt, M. B.; Gould, I. R. *J. Phys. Chem.* **1988**, *92*, 433 and references therein.

(7) (a) Johnson, R. C.; Merrifield, R. E. *Phys. Rev. B* **1970**, *1*, 896. (b) Avakian, P. *Pure Appl. Chem.* **1974**, *37*, 1. (c) Faulkner, L. R.; Bard, A. J. *J. Am. Chem. Soc.* **1969**, *91*, 209.

(8) Steiner, U. E.; Ulrich, T. *Chem. Rev.* **1989**, *89*, 51 and references therein.

Dynamics of an Oxazole Compound Bound to a Common Cold Virus

Wan F. Lau† and B. Montgomery Pettitt*,‡

Department of Chemistry, University of Houston
Houston, Texas 77204-5641

Received January 4, 1989

Due to the recent availability of crystal structures for one of the human rhinoviruses, HRV-14, with and without synthetic antiviral compounds bound to the protein coat,[1] it has become feasible to consider some of the macroscopic consequences of the binding of antivirals in terms of models of the microscopic interactions[2] and dynamics.[3] In this report, we focus on whether the dynamics of the antiviral drug itself when bound to the virial coat proteins are weakly coupled or strongly coupled to the dynamics of the protein and how this coupling is achieved. The oxazole antiviral compound we consider is 5-[7-[4-[(4,5-dihydro-4-methyl-2-oxazolyl)phenoxy]heptyl]-3-methylisoxazole. The results of our investigations may have implications for both

†Present address: Monsanto, St. Louis, MO.
‡Alfred P. Sloan Fellow 1989-1991.

(1) Smith, T. J.; Kremer, M. J.; Luo, M.; Vriend, G.; Arnold, E.; Kamer, G.; Rossman, M. G.; McKinlay, M. G.; Diana, G. D.; Otto, M. J. *Science* **1986**, *233*, 1286-1293.

(2) Lau, W. F.; Pettit, B. M.; Selective Elimination of Interactions: A method for Assessing Thermodynamic Contributions to Ligands Binding with Application to Rhinovirus Antivirals. *J. Med. Chem.*, in press.

(3) Lau, W. F.; Lybrand, T. P.; Pettitt, B. M. *Mol. Simulation* **1988**, *1*, 385-398.

0002-7863/89/1511-4111$01.50/0

future antiviral design studies as well as crystallographic refinement studies.

The virus, HRV-14, belongs to a relatively large family of rhinoviruses, one of the most important causative agents of the common cold. Molecular dynamics simulations were previously used in this laboratory to study the dynamics of a system consisting of an oxazole antiviral bound to the coat proteins of the human rhinovirus.[3] Parallel simulations were performed: one of the protein cluster consisting of four polypeptides that make up the protomeric unit and one of the ligand-bound cluster. We have reported from those simulations[3] the effects of the antiviral on the thermal vibrations and correlations in the coat proteins. Briefly, the ligand did not cause any statistically significant global changes in the amplitude of the atomic RMS fluctuations. For 17 residues close to the binding site, the drug caused the residues to move collectively and more in phase, as indicated from changes in the equal time cross-correlation functions of the residues. These results suggested a possible mechanical model for the effects of the drug on the dynamics of the coat protein. The ligand serves as a correlation linker between the individual residues, which can be thought of an independent, equivalent one-dimensional overdamped harmonic oscillators. We report here the effects of the protein on the dynamics of the drug itself by comparing the dynamics of the drug bound to the protein and the free drug.

The forces and the dynamics were calculated with the CHARMM program[4] using a force-field for the antiviral developed earlier.[5] The X-ray crystal structures[1] were energy refined, then heated to 300 K in a few picoseconds, and equilibrated for at least 10 more picoseconds before collecting the 10 ps trajectory for both the entire drug bound complex and the simulation of the free ligand. The relatively short time length was chosen to match the length of the trajectory for the protein ligand complex.[3] The simulations were performed in the NVE (microcanonical) ensemble and while of modest duration were useful for studying some coarse-grained quantities.

The thermal ellipsoids of the bound and the free ligand are indicated in Figure 1. The plots demonstrate the large thermal motion on the alkyl chain of the isoxazole end of the bound drug, compared to that of the free drug. The enlarged thermal ellipsoids for the bound structure are due to the (time averaged) conformational changes over the duration of the run. When visualized with graphics, a moving king/anti-kink wave is observed on the alkyl chain of the bound form. This wave must sum to zero at the end points that anchor it in the protein. However, the motion or displacement wave appears to spend more time at the isoxazole end of the chain than at the other. This motion is absent in the dynamics of the free drug. The alkane carbons rock around the chain, and no dihedral transitions are observed. This results in small RMS displacements and, thus, smaller thermal ellipsoids (see Figure 1) in vacuo. Two limiting descriptions of the dynamics are possible. One form is the strong coupling limit where the viral protein motions dominate the motions of the ligand. This picture is certainly valid for the overall translation and rotation of the bound ligand but fails to account for the conformational (intramolecular) dynamics. The alternative is a weak coupling limit where the protein serves as an environmental bath for the ligand, not unlike a solvent bath. The center chain portion of this flexible ligand seems to fit such a weak coupling picture with the proviso that the ends of the molecule are firmly (strongly) anchored in the protein matrix.

It is a combination of two condensed phase phenomena that is responsible for this drastic change in the motional behavior of the antiviral's alkane chain.[6] In terms of the intramolecular free energy surface, the intrinsic barriers to dihedral rotation are probably somewhat diminished for the bound alkane chain versus the same chain in vacuo. The motions of protein atoms, especially

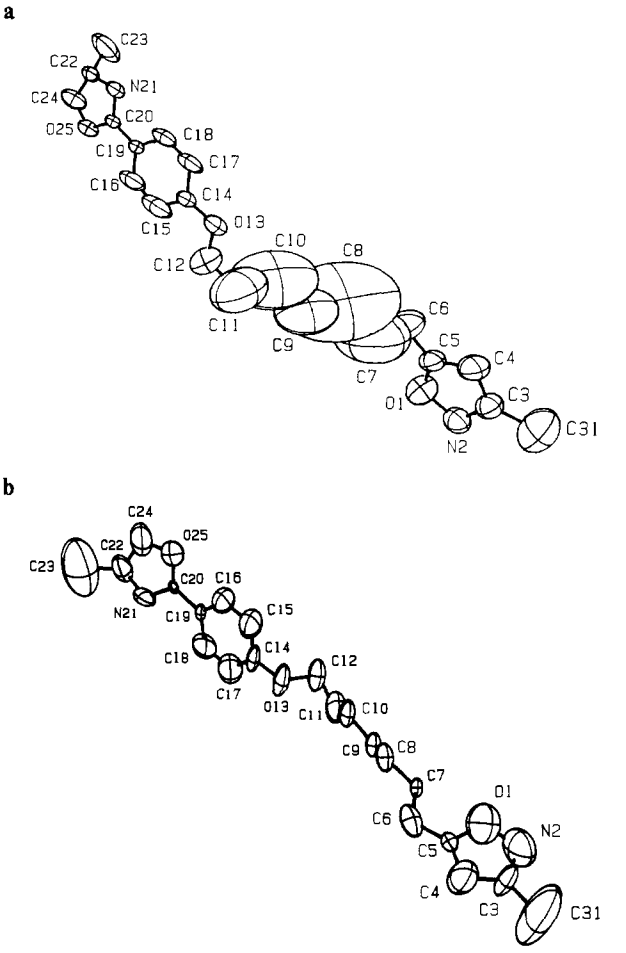

Figure 1. 5-[7-[4-(4,5-Dihydro-4-methyl-2-oxazolyl)phenoxy]heptyl]-3-methylisoxazole. (a) Structure and thermal elipsoids for the protein bound antiviral compound. (b) Structure and thermal elipsoids for the free (vacuum) antiviral compound.

in the vicinity of loop structures such as the FMDV loop in HRV-14, have, in many cases, been demonstrated to be quite fluid-like on short time scales.[6] It is well-known that dense liquids, particularly associated liquids, change the size of the effective barriers for dihedral transition in alkanes.[7,8] Thus, the viral protein coat may serve as a condensed phase environment reducing the intramolecular rotational barriers.

In addition, the actual barrier crossing may be thought of as an activated kinetic process. Here the protein coat serves as both a source and a sink for the kinetic energy of the dihedral degrees of freedom. In a Langevin-like analogy, the protein coat provides a thermal bath with a balance between "random" forces and friction to activate the actual dihedral transitions.[6,8]

The protein–drug interaction compared to that for separated species in vacuum is 27 kcal/mol.[2] While this is not really a binding energy difference per se, it is indicative of certain microscopic interactions. The van der Waals surface of the binding site indicates a large number of close contacts between the drug and the ligand, with little vacant volume or solvent exposure. This enables the drug to serve as a dynamic linker between residues, as discussed earlier. On the other hand, the protein "clamps" down on the two heterocyclic ends of the drug, i.e., the oxazole-phenoxy end and the isoxazole end, with hydrogen bonds and dipole forces limiting the motions of these two ends to relatively small thermal vibrations. Strain in the alkyl chain cannot be relieved via rotation of these ends in the bound state. The protein causes the ligand

(4) Brooks, B. R.; Bruccoleri, R. E.; Olafson, B. D.; States, D. J.; Swaminathan, S.; Karplus, M. *J. Comput. Chem.* **1983**, *4*8 187–217.
(5) Lybrand, T. P.; Lau, W. F.; McCammon, J. A.; Pettitt, B. M. *UCLA Symp. Mol. Cell. Biol.* **1987**, *69*, 227–233.
(6) Brooks, C. L.; Karplus, M.; Pettitt, B. M. *Adv. Chem. Phys.* **1988**, *71*, 1.
(7) Pratt, L. R.; Hsu, C. S.; Chandler, D. *J. Chem. Phys.* **1978**, *68*, 4202–4212.
(8) Montgomery, J. A., Jr.; Chandler, D.; Berne, B. S. *J. Chem. Phys.* **1979**, *70*, 4056–4066.

to maintain a somewhat bowed structure.[1]

The above results, which indicate a large disorder in the bound alkyl chain, offer an explanation for the difficulty in building the alkane chain into the crystallographic structure for a difference map.[9] The computed disorder shows a plausible density distribution that nearly has inversion symmetry and even in the crystallographic data, while the drug is slightly bent a near 2-fold symmetry of the electron density is visible.[9] The isoxazole and oxazole groups are quite similar dynamically. However, with the motion of the alkyl chain at the isoxazole end, which appears to sweep out a volume similar to the phenoxy group, the *thermal* volume traced out by the entire molecule is almost symmetrical (see Figure 1). Such a conformational equilibrium superimposed on a binding equilibrium involving a swap of one end for the other accounts for the difficulty in assigning the orientation of the ligand.[9] These motions would then have a direct effect on the binding equilibrium and, therefore, efficacy of the drug.

Acknowledgment. We appreciate many conversations with Professors T. Lybrand, J. A. McCammon, and Dr. A. Tresurywalla. We also thank Prof. M. Rossmann and Dr. J. Badger for communicating X-ray coordinates prior to publication. We thank the Sterling-Winthrop Research Institute, NIH, and the Robert A. Welch Foundation for partial financial support of this work. In addition, we acknowledge a grant of computing time from the San Diego Supercomputing facility as well as the use of our departmental VAX/FPS system, initially purchased with an NSF grant.

(9) Badger, J.; Minor, I.; Kremer, M. J.; Oliveira, M. A.; Smith, T. J.; Griffith, J. P.; Guerin, D. M. A.; Krishnaswamy, S.; Luo, M.; Rossmann, M. G.; McKinlay, M. A.; Diana, G. D.; Dutko, F. J.; Fancher, M.; Rueckert, R. R.; Heinz, B. A. *Proc. Natl. Acad. Sci. U.S.A.* **1988**, *85*, 3304-3308, and private communications with the authors.

Enantioselective Transport through a Silicone-Supported Liquid Membrane

William H. Pirkle* and Elizabeth M. Doherty

School of Chemical Sciences
University of Illinois
Urbana, Illinois 61801

Received February 13, 1989

Tartaric acid derivatives,[1] chiral amine hydrochlorides,[2] chiral crown ethers,[3] and cyclodextrins[4] previously have been utilized as transport agents in enantioselective liquid membranes. To be of practical utility, chiral transport agents must be relatively inexpensive and afford high levels of enantioselectivity. One of the chiral selectors developed in our laboratory[5] meets these requirements and has been used in a single stage bench top prototype membrane device which is capable of affording significant enantiomeric enrichment for appreciable quantities of material.

When swollen with solvent, silicone rubber tubing (Dow-Corning medical grade 0.063 o.d. × 0.030 i.d.) is permeable to even moderately large organic compounds. The membrane device

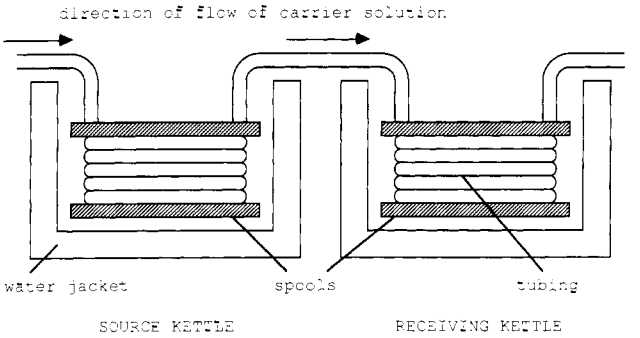

Figure 1. Diagram of the prototype membrane device. The temperature-controlled source and receiving phases are stirred magnetically, while the (*S*)-*N*-(1-naphthyl)leucine octadecyl ester–dodecane solution is slowly recirculated (pump not shown) through the silicone rubber tubing.

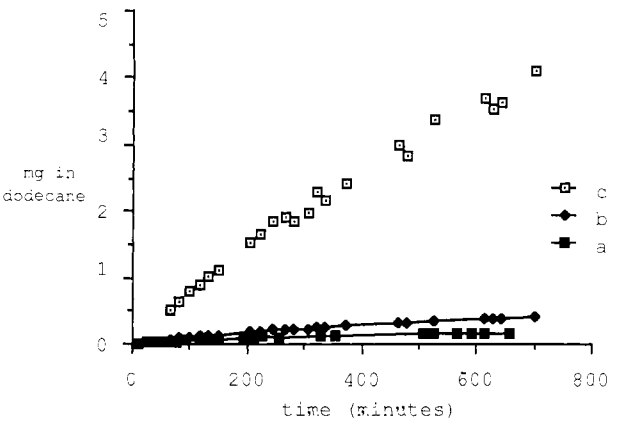

Figure 2. The amount of *N*-(3,5-dinitrobenzoyl)leucine butyl ester present in the dodecane phase (5 mL) as the run progresses. Curve a: no chiral transport agent present. This curve represents each enantiomer. Curve b: The (*R*)-enantiomer when 100 mg of the (*S*)-transport agent has been added to the dodecane. Curve c: The (*S*)-enantiomer when 100 mg of the (*S*)-transport agent has been added to the dodecane.

(Figure 1) consists of 8 ft of tubing wrapped about two spools, each spool being immersed in separate temperature-controlled baths containing 4:1 methanol–water (50 mL). Dodecane (5 mL) is pumped slowly (1 mL/min) through the tubing in a recycle mode. The analyte (50 mg of a racemic *N*-(3,5-dinitrobenzoyl)α-amino ester or amide) is dissolved in the (upstream) source kettle and diffuses slowly through the walls of the tubing. Once in the dodecane solution, the analyte is swept downstream where it can diffuse into the methanol–water in the receiving kettle. The rate of this achiral transport is quite slow; the rate of entry into the dodecane solution at 18 °C is shown in Figure 2.[6] When (*S*)-*N*-(1-naphthyl)leucine octadecyl ester (100 mg) is added to the dodecane, it impregnates the tubing walls, and the rate of transport into the dodecane solution increases. For example, at 18 °C the (*S*)-enantiomer of *N*-(3,5-dinitrobenzoyl)leucine *n*-butyl ester enters the dodecane nine times faster than does the (*R*)-enantiomer. This ratio encompasses both the achiral and the facilitated transport processes (Figure 2). When swept downstream, the analyte diffuses into the 18 °C receiver phase in a 4:1 (*S*):(*R*) ratio; this again represents the summation of the achiral and the chiral transport processes. Here, the presence of the enantioselective transport agent in the dodecane works against the scrubbing process.

Table I presents information concerning the initial rates at which a number of analyte enantiomers were transported into the methanol–water receiving phase when the source and receiving kettles were maintained at 18 °C. Both absolute and relative rates

(1) Prelog, V.; Dumic, M. *Helv. Chim. Acta* **1986**, *69*, 5-11.
(2) Lehn, J. M.; Moradpour, A.; Behr, J. P. *J. Am. Chem. Soc.* **1975**, *97*, 2532, 2534.
(3) (a) Newcomb, M.; Toner, J. L.; Helgeson, R. C.; Cram, D. J. *J. Am. Chem. Soc.* **1979**, *101*, 4941-4947. (b) Nakazaki, M.; Yamamoto, K.; Tetsumi, I.; Kitsuki, T.; Okamoto, Y. *J. Chem. Soc., Chem. Commun.* **1983**, 787-788. (c) Yamamoto, K.; Noda, K.; Okamoto, Y. *J. Chem. Soc., Chem. Commun.* **1985**, 1065-1066. (d) Yamamoto, K.; Fukushima, H.; Okamoto, Y.; Hatada, K.; Nakazaki, M. *J. Chem. Soc., Chem. Commun.* **1984**, 1111-1112. (e) Naemura, K.; Fukunaga, R. *Chem. Lett.* **1985**, 1651-1654. (f) Naemura, K.; Fukunaga, R.; Yamanoka, M. *J. Chem. Soc., Chem. Commun.* **1985**, 1560-1561. (g) Naemura, K.; Ebashi, I.; Matsuda, A.; Chikamatsu, H. *J. Chem. Soc., Chem. Commun.* **1986**, 666-668. (i) Yamaguchi, T.; Nishimura, K.; Shinbo, T.; Sugiura, M. *Chem. Lett.* **1985**, 1549-1552.
(4) Armstrong, D. W.; Jin, H. L. *Anal. Chem.* **1987**, *59*(*18*), 2237-2241.
(5) Selectors of this type were first prepared in these laboratories by Kris C. Deming for use as a chiral stationary phase for liquid chromatography.

(6) Aliquots of the various phases were analyzed by HPLC using an (*R*)-*N*-(2-naphthyl)alanine-derived CSP of 33% ee. The reduced ee retards the initially eluted (*S*)-analyte and hastens the elution of the (*R*)-analyte, hastening analysis and ensuring more accurate electronic integration.

0002-7863/89/1511-4113$01.50/0